Surface Termination of Cleaved Bi$_2$Se$_3$ Investigated by Low Energy Ion Scattering

X. He,[1] W. Zhou,[1] Z. Y. Wang,[1] Y. N. Zhang,[2] J. Shi,[1] R. Q. Wu,[2] and J. A. Yarmoff[1,*]

[1]*Department of Physics and Astronomy, University of California, Riverside, California 92521, USA*
[2]*Department of Physics and Astronomy, University of California, Irvine, California 92697, USA*

It has been widely assumed that Se terminates the surface of the topological insulator, bismuth selenide. Although some Se is initially at the surface after cleaving at 80 K, low energy ion scattering reveals a complete Bi termination at room temperature. Density functional theory shows that a Bi bilayer atop the bulk-terminated structure is energetically favorable. It is thus proposed that a thermally activated process induces a spontaneous termination change after cleaving. This has profound implications on the electrical transport and long-term stability of such materials and devices.

The (Bi, Sb)$_2$(Te, Se)$_3$ family of compounds possesses novel electronic phases involving gapless topological insulator (TI) surface states [1–4]. These states, characterized by a Dirac cone, represent a new type of two-dimensional electron gas in which the electron's spin is locked to its linear momentum [5]. TI materials have attracted intense interest because of their fundamental importance and their great potential for applications in spintronics and quantum computation [6–8].

The prototypical compound in this family, bismuth selenide (Bi$_2$Se$_3$), is a degenerate n-type semiconductor in which the topological surface states coexist with an overwhelmingly large number of bulk states. By adding p-type dopant atoms to compensate for the natural n-type doping [2,9–11], the bulk can become insulating so that surface transport dominates, although the surface can still significantly differ from the bulk due to band bending [12]. A critical issue in applications of TI materials is a time-dependent change in surface electronic states revealed by angle-resolved photoelectron spectroscopy (ARPES). This "aging effect" makes the surface transport rather uncontrollable [2,13,14].

The physical origin of the time-dependent effects is not yet understood. Since selenium (Se) has a relatively high vapor pressure, it has often been assumed that the natural n-type doping and band bending result from the development of near-surface Se vacancies. Surface contamination by water or carbon monoxide [14–16] and slow interlayer relaxations [13] have also been suggested as causes. To make use of the Dirac surface state, it is crucial to establish a clear understanding of the surface morphology and stability of TIs.

In this Letter, low energy ion scattering (LEIS) measurements and density functional theory (DFT) calculations indicate that a surface reconstruction mechanism might be the underlying cause of the slow deterioration. LEIS is especially sensitive to the elemental identity and atomic structure of the outermost atomic layers of a solid [17]. After *in situ* cleaving of Bi$_2$Se$_3$(111) in ultrahigh vacuum (UHV) at room temperature, it is shown that the outermost atomic layer contains only bismuth (Bi) with no detectable Se. DFT shows that it is energetically favorable for an additional Bi bilayer to sit atop the nominal bulk-terminated quintuple layer (QL) structure, and that the TI surface states are protected in this configuration.

Techniques used in previous surface studies do not directly identify the outermost surface atoms. For example, scanning tunneling microscopy (STM) [18–21] shows atomic scale features, but cannot identify the specific species. ARPES provides a surface sensitive measure of the band structure of the material [2,5,9,12], but this is not an identification of the atomic structure. Ion scattering is one of the few techniques that gives an unambiguous measure of the elemental composition at a surface.

The expectation of a Se-termination is derived from the bulk crystal structure. Bi$_2$Se$_3$ has a rhombohedral unit cell that forms a layered material with a basic QL unit composed of five atomic layers ordered as Se-Bi-Se-Bi-Se. While the atoms within each QL are held together by strong covalent-type bonds, the QLs are attached to each other by relatively weak van der Waals-type bonds. It is therefore natural to assume a cleavage plane between two QLs that would result in a Se termination [1,2,5,9,12,18–22]. The present LEIS measurements appear to contradict this simple picture, however, and show that the structural properties of TI surfaces need to be revisited.

Single crystals of Bi$_2$Se$_{3.12}$ were grown using a multi-step heating method [10]. High-purity Bi (99.999%) and Se (99.999%) were mixed stoichiometrically and sealed in an evacuated quartz tube. The tube was heated to 1020 K for 4 h, cooled to and kept at 870 K for 5 d, and then cooled to room temperature. It was next heated to 970 K for ~15 h and finally cooled to room temperature naturally. The high quality single crystallinity was confirmed with x-ray diffraction. The measured band gap, reduced effective mass of charge carriers, and carrier density and mobility are all consistent with expectations for a TI material [23].

LEIS and low energy electron diffraction (LEED) were performed in two separate UHV chambers with load-locks that enable rapid introduction of samples without the need for bakeout. One of the LEIS chambers allows for variation of the azimuthal orientation and scattering angle. The other contains a cryogenic sample manipulator, but the scattering angle is fixed at $\theta = 150°$ and the azimuthal orientation cannot be adjusted. In this chamber, LEED is used to determine the orientation along which the sample is mounted.

LEIS was performed as described previously [24,25]. The Na^+ beam was pulsed at 80 kHz and incident along the surface normal. The backscattered projectiles were detected by a triple microchannelplate array after traveling through a drift tube. The flight times are histogrammed to obtain time-of-flight (TOF) spectra. The total yield of scattered ions and neutrals are collected so that neutralization need not be considered. To minimize beam damage and insure that the data reflect the unperturbed material, the fluence was kept to less than 1×10^{12} ions cm^{-2}, which is an order of magnitude below where damage is observed.

The samples were cleaved *in situ*, using a procedure [24] that results in a flat and shiny appearance. The observed 1×1 LEED pattern indicates a clean and well-ordered surface. X-ray photoelectron spectroscopy (XPS) and STM were performed in separate instruments following *in situ* cleaving of samples from the same batch. XPS showed no evidence for oxidation of either Bi or Se [26], while STM showed a smooth surface with atomically resolved features [18–21].

LEIS spectra contain a single scattering peak (SSP) for each elemental species at the surface, as the kinetic energy of a singly scattered ion depends on the mass of the target atom [17]. Figure 1 shows a TOF spectrum for 3.0 keV ^{23}Na$^+$ scattered at $\theta = 125°$ from cleaved Bi$_2$Se$_3$(111). The polar emission angle $\alpha = 35°$ is with respect to the sample plane, and the azimuthal orientation $\phi = 0°$ is with respect to the projection along the [$\bar{1}$10] direction. The only feature in the spectrum is the Bi SSP at $\sim$2.1 keV, which corresponds to a Na projectile scattered directly from a surface Bi atom. The Bi SSP rides on a broad background of multiply scattered projectiles. The Se SSP would be expected at $\sim$1.1 keV, but is completely absent.

The SSP intensity reflects the number of surface atoms directly visible to both the incoming ion beam and the detector, but is further dependent on shadowing, blocking and focusing as the projectile interacts with other atoms along the trajectory [17,27]. A shadow cone is the region behind a surface atom from which incident projectiles are excluded. A blocking cone is a similar notion, but is the region above a surface atom from which an exiting projectile is excluded following scattering from a deeper atom. Focusing occurs when the edge of a shadow cone intersects an atomic position or the edge of a blocking cone is pointing towards the detector, as the flux is increased at
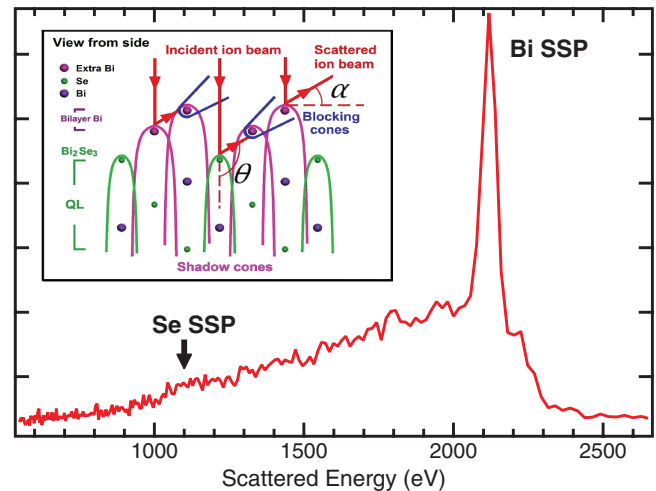

FIG. 1 (color). TOF spectrum, after conversion to an energy scale, for normally incident 3.0 keV Na^+ scattered from Bi$_2$Se$_3$ cleaved at room temperature. The scattered projectiles were emitted at a polar angle of $\alpha = 35°$ with respect to the surface plane (scattering angle $\theta = 125°$) and the projection of the azimuthal angle was along $\phi = 0°$. The inset shows a schematic side view of Bi$_2$Se$_3$(111) indicating the shadow (purple and green) and blocking (blue) cones for the orientation employed. This diagram assumes that there is an extra Bi bilayer above the nominal QL of bulk Bi$_2$Se$_3$.

the edge of a cone. As the sample orientation is adjusted with respect to the incoming beam or detector, changes in the alignment of cones with atoms in the crystal structure lead to changes in the SSP intensities. These variations are commonly exploited to determine the near-surface atomic structure of a single crystal material [27,28].

Shadowing and blocking can be used to provide a geometry that is sensitive to only the outermost atomic layer. The inset to Fig. 1 shows a schematic side view of the shadow and blocking cones in relation to the Bi$_2$Se$_3$(111) crystal structure for the geometry employed here. With normal incidence, atoms below the top three layers are completely shadowed from the incident beam. By positioning the detector at $\phi = 0°$, projectiles that would backscatter from second and third layer atoms are blocked from directly reaching the detector. This is a "double alignment" orientation in which only projectiles scattered from the outermost atomic layer can exit at the SSP energy. Although the diagram shows the surface in which the nominal QL is capped by a Bi bilayer, the concept would be the same with only a single Bi layer. Conversely, if Se were terminating the surface, then only the Se SSP would be visible.

The absence of a Se SSP is compelling evidence that Bi is the only element in the outermost atomic layer of Bi$_2$Se$_3$(111) after cleaving at room temperature. Preliminary molecular dynamics simulations, using the KALYPSO package [29], confirm that a Bi-terminated structure would lead to the complete absence of a Se SSP in this

orientation. A more thorough analysis of the angular distributions of the scattered yields, in conjunction with additional simulations, is underway to confirm the surface structure. Nonetheless, the absence of the Se SSP can only be reconciled with a model in which the outermost surface is completely Bi.

To produce a Bi-terminated structure, it is possible that the material initially cleaves between QL's, forming the expected Se termination, but the termination then changes via atomic diffusion or desorption. If this were the case, a low temperature may slow down the process so that it could be monitored in real time.

To investigate this possibility, a sample was cooled to 80 K with liquid nitrogen prior to cleaving, and LEIS spectra were collected while maintaining the low temperature. Multiple cleaves were performed from the same crystal at a fixed azimuth so that measurements at the two temperatures could be directly compared. The insets to Fig. 2 show spectra collected at the indicated times since cleaving. Note that a double alignment configuration could not be used because the low temperature chamber does not allow for azimuthal adjustment. In the orientation employed, the normally incident ions impact the first three atomic layers. Since each spectrum shows a small Se SSP, it can be concluded that Se is present in the second or third atomic layer. Note that the relative intensities of the SSP's do not quantitatively reflect their abundance, however, due to secondary effects that include differences in scattering cross section, changes in detector sensitivity with scattered energy, and focusing.
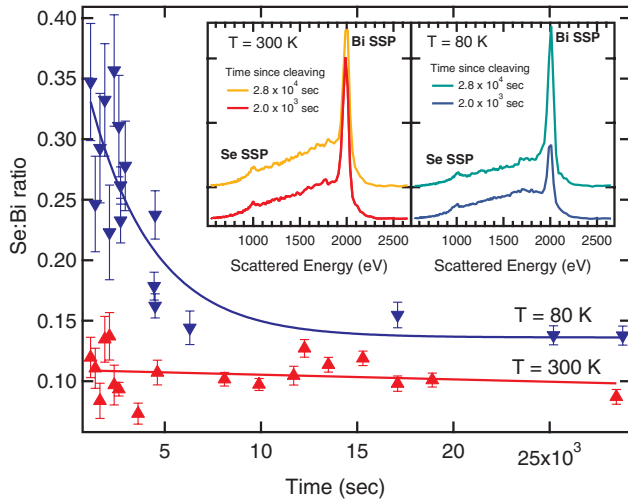

FIG. 2 (color). The raw Se:Bi SSP ratios derived from TOF spectra for 3.0 keV Na$^+$ ions scattered at $\theta = 150°$ from cleaved Bi$_2$Se$_3$ at an azimuthal orientation of $\phi = -12.5°$ after cleaving at the indicated temperature, shown as a function of time since cleaving. The solid blue line is an exponential fit to the 80 K data while the solid red line is a linear fit to the 300 K data. Insets: Raw total yield TOF spectra collected the indicated time after cleaving and maintaining at the indicated temperature.

A comparison of the time evolution of the Se and Bi SSPs at the two temperatures provides evidence that the termination does change. Figure 2 plots the raw Se:Bi SSP ratios as a function of time since cleaving, determined via background subtraction and integration. At 300 K, the Se:Bi ratio is ~0.10 and fairly constant. At 80 K, however, the Se:Bi ratio starts at about 0.35 and drops gradually to 0.14, which is close to the room temperature value. An exponential fit to the data gives a time constant of 2775 sec. This suggests that Se is present at the surface immediately after cleaving at low temperature but the termination changes over time, while at room temperature the change is too fast to be observed.

Although this temperature dependence suggests that the termination change is thermally activated, the specific process cannot be determined from these data. Se is a volatile element with a relatively high vapor pressure, so that the termination change could involve Se evaporation in the form of gas-phase dimers or tetramers. Another possibility, however, is the accumulation of additional Bi at the surface via diffusion from the bulk. Such diffusion could involve Bi intercalating between the van der Waals layers, with the driving force being the surfactant properties of Bi. Surfactants are elements with low solid solubilities that collect at a surface to reduce the overall surface energy, and are stable even with a large lattice mismatch and strain [30,31]. The behavior of Bi as a surfactant is well documented in the thin film growth literature [24,32–35].

DFT calculations were performed to evaluate the stability of various Bi$_2$Se$_3$(111) structures using the Vienna *ab initio* simulation package (VASP) [36] along with the projector augmented wave method [37]. The generalized-gradient approximation [38] described the exchange-correlation interaction among electrons. The surface was modeled as a periodic slab with a (1×1) unit cell in the lateral plane for most cases and a (2×1) unit cell for intermixed surfaces, and 5 QLs per slab separated by an ~18 Å vacuum along the surface normal. The lateral lattice constant was fixed to that of the bulk, $a = 4.14$ Å [22,39]. While atoms in the 11 interior layers were frozen at their bulk positions, others were relaxed until forces on them became smaller than 0.01 eV Å^{-1}. An energy cutoff of 350 eV was used for the plane-wave basis expansion, and an $11 \times 11 \times 1$ k-point mesh in the Brillouin zone was used for k-space integrations. Spin-orbit coupling (SOC) was self-consistently invoked.

Eight different Se, Bi, and mixed terminations were investigated. The stability of each structure is quantitatively described by its surface energy as

$$\gamma = (E_{surf} - n_{Bi}\mu_{Bi} - n_{Se}\mu_{Se})/2A, \qquad (1)$$

where E_{surf} is the total energy of the slab, A is the surface area, and n_{Bi} and n_{Se} represent the numbers of Bi and Se atoms, respectively. The chemical potential of a Bi atom, μ_{Bi}, was used as the variable while the chemical potential
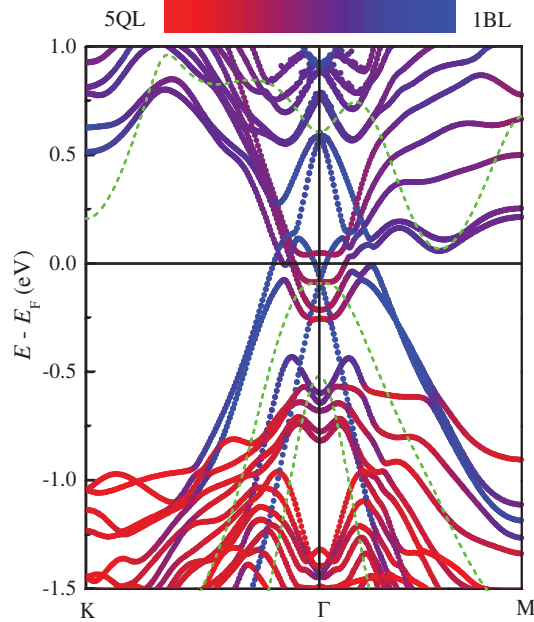
FIG. 3 (color). Calculated band structure of a Bi bilayer atop bulk-terminated Bi_2Se_3(111). The color scale indicates the contributions from the surface Bi bilayer (blue) and the underlying Bi_2Se_3 QL's (red). The green dashed lines are the bands of a free Bi bilayer.

of Se, μ_{Se}, was calculated via the constraint: $2\mu_{Bi} + 3\mu_{Se} = \mu_{Bi2Se3}$. Here, μ_{Bi2Se3} is the chemical potential (or total energy at 0 K) of one bulk Bi_2Se_3 unit. To mimic different environments, a broad range is set for μ_{Bi}, from -2.10 eV with bulk Bi as the reservoir (Bi-poor), to 0.0 eV with isolated Bi atoms as the reservoir (Bi-rich). With the inclusion of a van der Waals correction, the calculated surface energy of the generic Bi_2Se_3(111) surface is only 0.18 J/m^2, indicating its rather inert nature.

Significantly, all the explored Bi-terminated surfaces are more stable than other Bi_2Se_3 surfaces in Bi-rich conditions. In particular, the structure in which a complete Bi (111) bilayer is atop the nominal Bi_2Se_3 QL is the most stable over almost the entire range of μ_{Bi}, suggesting that this is likely the structure observed in the measurements. Note that the bilayer is compressed since the lateral constant of a freestanding Bi bilayer is larger than that of Bi_2Se_3(111), 4.54 vs. 4.14 Å. The interlayer distance between the Bi and Bi_2Se_3 is 3.05 Å, which is larger than the distance between adjacent QLs (2.57 Å). Therefore, the interaction between the Bi adlayer and Bi_2Se_3 is rather weak and the structure would be even more stable if incommensurate matching were allowed.

As expected, the topological surface states persist in the presence of the Bi bilayer, as seen in the calculated band structure of Fig. 3. Their weights in the bilayer and the Bi_2Se_3 substrate are highlighted in blue and red, respectively. Interestingly, the characteristic Dirac surface states disappear from bands associated with the QL's (red lines).

Instead, a new Dirac cone develops in the Bi adlayers just below the Fermi energy (blue lines). Clearly, the Dirac states are topologically protected and may ''float'' to the topmost layers, as reported for Au/Bi_2Se_3(111) [40] and in the presence of surface contamination [41]. As a result, ARPES would mainly see a Dirac cone. Because of a small amount of charge transfer from Bi, the first QL has several conducting bands that intercept the Fermi level. Nevertheless, these bands might not be observable in ARPES due to screening by the Bi bilayer. It should be stressed that the Dirac states are not solely from the Bi bilayer since the band structure of a free bilayer (green dashed lines) has an insulating character. Similar features were also reported for a Bi bilayer grown atop Bi_2Te_3, but the enhanced stability of the bilayer was not discussed [42].

In summary, LEIS reveals a Bi-terminated surface after *in situ* cleaving of Bi_2Se_3(111) at room temperature. Cleaving at low temperature reveals a thermally activated process whereby the termination switches from Se to Bi. DFT shows that a Bi bilayer-terminated crystal is particularly stable, and that the TI surface states are protected. This termination change may explain time-dependent effects that have been reported for these materials.

*Corresponding author.
yarmoff@ucr.edu

[1] H. Zhang, C.-X. Liu, X.-L. Qi, X. Dai, Z. Fang, and S.-C. Zhang, Nat. Phys. **5**, 438 (2009).

[2] D. Hsieh, Y. Xia, D. Qian, L. Wray, J. H. Dil, F. Meier, J. Osterwalder, L. Patthey, J. G. Checkelsky, N. P. Ong, A. V. Fedorov, H. Lin, A. Bansil, D. Grauer, Y. S. Hor, R. J. Cava, and M. Z. Hasan, Nature (London) **460**, 1101 (2009).

[3] Y. L. Chen, J. G. Analytis, J. H. Chu, Z. K. Liu, S. K. Mo, X. L. Qi, H. J. Zhang, D. H. Lu, X. Dai, Z. Fang, S. C. Zhang, I. R. Fisher, Z. Hussain, and Z. X. Shen, Science **325**, 178 (2009).

[4] Z. Alpichshev, J. G. Analytis, J. H. Chu, I. R. Fisher, Y. L. Chen, Z. X. Shen, A. Fang, and A. Kapitulnik, Phys. Rev. Lett. **104**, 016401 (2010).

[5] M. Bianchi, D. D. Guan, S. N. Bao, J. L. Mi, B. B. Iversen, P. D. C. King, and P. Hofmann, Nat. Commun. **1**, 128 (2010).

[6] L. Fu and C. L. Kane, Phys. Rev. Lett. **100**, 096407 (2008).

[7] X. L. Qi, R. D. Li, J. D. Zang, and S. C. Zhang, Science **323**, 1184 (2009).

[8] A. M. Essin, J. E. Moore, and D. Vanderbilt, Phys. Rev. Lett. **102,** 146805 (2009).

[9] K. Kuroda, M. Arita, K. Miyamoto, M. Ye, J. Jiang, A. Kimura, E. E. Krasovskii, E. V. Chulkov, H. Iwasawa, T. Okuda, K. Shimada, Y. Ueda, H. Namatame, and M. Taniguchi, Phys. Rev. Lett. **105,** 076802 (2010).

[10] Z. Wang, T. Lin, P. Wei, X. Liu, R. Dumas, K. Liu, and J. Shi, Appl. Phys. Lett. **97,** 042112 (2010).

[11] J. G. Analytis, R. D. McDonald, S. C. Riggs, J.-H. Chu, G. S. Boebinger, and I. R. Fisher, Nat. Phys. **6,** 960 (2010).

[12] J. G. Analytis, J. H. Chu, Y. L. Chen, F. Corredor, R. D. McDonald, Z. X. Shen, and I. R. Fisher, Phys. Rev. B **81,** 205407 (2010).

[13] H. J. Noh, H. Koh, S. J. Oh, J. H. Park, H. D. Kim, J. D. Rameau, T. Valla, T. E. Kidd, P. D. Johnson, Y. Hu, and Q. Li, Europhys. Lett. **81,** 57 006 (2008).

[14] P. D. C. King, R. C. Hatch, M. Bianchi, R. Ovsyannikov, C. Lupulescu, G. Landolt, B. Slomski, J. H. Dil, D. Guan, J. L. Mi, E. D. L. Rienks, J. Fink, A. Lindblad, S. Svensson, S. Bao, G. Balakrishnan, B. B. Iversen, J. Osterwalder, W. Eberhardt, F. Baumberger, and P. Hofmann, Phys. Rev. Lett. **107,** 096802 (2011).

[15] H. M. Benia, C. Lin, K. Kern, and C. R. Ast, Phys. Rev. Lett. **107,** 177602 (2011).

[16] M. Bianchi, R. C. Hatch, J. L. Mi, B. B. Iversen, and P. Hofmann, Phys. Rev. Lett. **107,** 086802 (2011).

[17] J. W. Rabalais, *Principles and Applications of Ion Scattering Spectrometry: Surface Chemical and Structural Analysis* (Wiley, New York, 2003).

[18] S. Urazhdin, D. Bilc, S. H. Tessmer, S. D. Mahanti, T. Kyratsi, and M. G. Kanatzidis, Phys. Rev. B **66,** 161306 (R) (2002).

[19] S. Urazhdin, D. Bilc, S. D. Mahanti, S. H. Tessmer, T. Kyratsi, and M. G. Kanatzidis, Phys. Rev. B **69,** 085313 (2004).

[20] Y. S. Hor, A. Richardella, P. Roushan, Y. Xia, J. G. Checkelsky, A. Yazdani, M. Z. Hasan, N. P. Ong, and R. J. Cava, Phys. Rev. B **79,** 195208 (2009).

[21] Z. Alpichshev, R. R. Biswas, A. V. Balatsky, J. G. Analytis, J. H. Chu, I. R. Fisher, and A. Kapitulnik, Phys. Rev. Lett. **108,** 206402 (2012).

[22] W. Zhang, R. Yu, H.-J. Zhang, X. Dai, and Z. Fang, New J. Phys. **12,** 065013 (2010).

[23] P. Wei, Z. Wang, X. Liu, V. Aji, and J. Shi, Phys. Rev. B **85,** 201402 (2012).

[24] R. D. Gann, J. Wen, Z. Xu, G. D. Gu, and J. A. Yarmoff, Phys. Rev. B **84,** 165411 (2011).

[25] C. B. Weare and J. A. Yarmoff, Surf. Sci. **348,** 359 (1996).

[26] D. S. Kong, J. J. Cha, K. J. Lai, H. L. Peng, J. G. Analytis, S. Meister, Y. L. Chen, H. J. Zhang, I. R. Fisher, Z. X. Shen, and Y. Cui, ACS Nano **5,** 4698 (2011).

[27] Th. Fauster, Vacuum **38,** 129 (1988).

[28] H. Niehus, W. Heiland, and E. Taglauer, Surf. Sci. Rep. **17,** 213 (1993).

[29] M. A. Karolewski, Nucl. Instrum. Methods Phys. Res., Sect. B **230,** 402 (2005).

[30] P. G. de Gennes, Rev. Mod. Phys. **57,** 827 (1985).

[31] M. Copel, M. C. Reuter, E. Kaxiras, and R. M. Tromp, Phys. Rev. Lett. **63,** 632 (1989).

[32] K. Sakamoto, H. Matsuhata, K. I. Kyoya, K. Miki, and T. Sakamoto, Jpn. J. Appl. Phys., Part 1 **33,** 2307 (1994).

[33] K. Miki, J. H. G. Owen, D. R. Bowler, G. A. D. Briggs, and K. Sakamoto, Surf. Sci. **421,** 397 (1999).

[34] S. W. Jun, C. M. Fetzer, R. T. Lee, J. K. Shurtleff, and G. B. Stringfellow, Appl. Phys. Lett. **76,** 2716 (2000).

[35] H. B. Naceur, T. Mzoughi, I. Moussa, L. Nguyen, A. Rebey, and B. El Jani, Physica (Amsterdam) **43E,** 106 (2010).

[36] G. Kresse and J. Furthmüller, Comput. Mater. Sci. **6,** 15 (1996).

[37] P. E. Blöchl, Phys. Rev. B **50,** 17 953 (1994).

[38] J. P. Perdew, K. Burke, and M. Ernzerhof, Phys. Rev. Lett. **77,** 3865 (1996).

[39] H. Lind, S. Lidin, and U. Häussermann, Phys. Rev. B **72,** 184101 (2005).

[40] H. Chen, W. Zhu, D. Xiao, and Z. Zhang, Phys. Rev. Lett. **107,** 056804 (2011).

[41] Z. K. Liu, Y. L. Chen, J. G. Analytis, S. K. Mo, D. H. Lu, R. G. Moore, I. R. Fisher, Z. Hussain, and Z. X. Shen, Physica (Amsterdam) **44E,** 891 (2012).

[42] T. Hirahara, G. Bihlmayer, Y. Sakamoto, M. Yamada, H. Miyazaki, S.-I. Kimura, S. Blügel, and S. Hasegawa, Phys. Rev. Lett. **107,** 166801 (2011).